ISSN 0304-9892 (Print) ISSN 2455-7463 (Online)
www.vijnanaparishadofindia.org/jnanabha
***Jñānābha*, Vol. 53(2) (2023), 273-286**
(Dedicated to Professor V. P. Saxena on His 80^{th} *Birth Anniversary Celebrations)*

TAYLOR WAVELET APPROACH FOR THE SOLUTION OF THE FREDHOLM INTEGRO-DIFFERENTIAL EQUATION OF THE SECOND KIND

Vivek, Suyash Narayan Mishra and Manoj Kumar
Applied Sciences and Humanities Department, Institute of Engineering and Technology, Lucknow, Uttar Pradesh, India-226021
Email: vk35@iitbbs.ac.in, snmishra@ietlucknow.ac.in, manojkumar@ietlucknow.ac.in

(Received : March 13*,* 2023*; In format : March* 24*,* 2023*; Revised : December* 05*,* 2023*; Accepted : December* 08*,* 2023*)*

DOI: https://doi.org/10.58250/jnanabha.2023.53234

Abstract

A Taylor wavelet technique is used to obtain the approximate solution of the Fredholm integro-differential equations *(IDEs)* of the second kind. Taylor wavelet method is based on an estimate of the unknown function involved in a given *IDEs* using the Taylor wavelet basis. The simplicity of the technique is a highly striking feature for the estimate of the unknown function. The applicability of the technique on various numerical problems shows the preciseness and usefulness of the technique. The suggested wavelets approach stands out for its simple operations, easy implementation, and accurate answers. A comparison is made with previous findings.

2020 Mathematical Sciences Classification: 45D05, 45D99.
Keywords and Phrases: Taylor wavelet, Operational integration matrix, Collocation points, Integro-differential equation, MATLAB.

1 Introduction

Integral equations play a crucial role in various branches of mathematics, engineering, and the sciences. These equations involve the unknown function as part of the integrand, and they arise in diverse fields due to their ability to model a wide range of phenomena. Integral equations can be solved using a variety of analytical and numerical methods. The choice of method often depends on the specific characteristics of the integral equation and the problem at hand. Problems involving heat transfer and fluid dynamics often lead to integro-differential equations. These equations can describe the distribution of temperature or fluid velocity in a given domain, accounting for both differential effects (diffusion or convection) and integral effects (boundary interactions). Here are some common techniques used to handle integral equations including the series solution method, Adomian decomposition method (ADM) and its modification, variational iteration method (VIM), Homotopy perturbation method, Nystrm method, and so on. On the other hand, recently Kumar, Chandel, and Srivastava [11], discussed a fractional non-linear biological model problem and its approximation. Further Kumar [12] discussed a class of two variable sequence of functions satisfying Able's integral equation and phase shifts. Take into account the Fredholm integro-differential equation *(IDEs)* of the following form:

$$\begin{cases} \Lambda'(\rho) = h(\rho, \Lambda(\rho)) + \int_0^1 \kappa(\rho, \xi, \Lambda(\xi))d\xi, 0 \leq \rho \leq 1 \\ \Lambda(0) = \Lambda_0, \end{cases} \tag{1.1}$$

where $\Lambda(\rho)$ is the function(unknown) to be evaluated and $h(\rho, \Lambda(\rho)) \in L^2[0, 1]$ and the kernel $\kappa(\rho, \xi) \in L^2(\mathbb{R})$ are known functions. In this paper, we present a new estimate solution for the Fredholm integro-differential equation *(IDEs)* (1.1). In this study, we investigate a fresh unified method for the solution of the integral equations, where the integral equations are expanded in terms of the Taylor wavelet with unique coefficients, leading to the reduction of the integral equations to algebraic equations.

A wavelet is a waveform that is localized in both time and frequency domains, and it is often used in signal processing and the analysis of time-varying signals. Wavelets have the property that they start from zero, oscillate, and then return to zero, and they come in different shapes and sizes. In the context of wavelets, the term "oscillation" refers to the repetitive pattern or behavior of the wavelet. The amplitude of a wavelet may indeed start at zero, rise or fall, and return to zero, and this property is often desirable in applications where

a localized representation of a signal or function is needed. The ability of wavelets to capture both high and low-frequency components of a signal in a localized manner makes them well-suited for analyzing signals with complex and changing patterns. Multiresolution analysis (MRA), density, orthogonality, and compact support characteristics collectively make wavelets powerful tools in various fields, including signal processing, image compression, data analysis, and solving differential equations. The adaptability of wavelets to analyze signals at different scales, their ability to capture localized features, and their efficiency in representation and computation make them valuable tools in diverse scientific, engineering, and mathematical applications. Different types of wavelets are often chosen based on the specific requirements of the application at hand. Wavelet analysis is based on the concept of multiresolution analysis, meaning that it can represent a signal at different levels of detail or resolution. This is particularly useful for signals with non-stationary or time-varying characteristics.

Indeed, The use of orthogonal basis functions, especially in the form of orthogonal wavelet bases, has played a crucial role in the success and widespread adoption of wavelet analysis in numerical applications. The orthogonality property enhances the efficiency, stability, and accuracy of numerical procedures involving wavelet transformations. Wavelet basis functions lead to a sparse representation of signals. This sparsity often allows for a significant reduction in the number of coefficients needed to represent a signal accurately. As a result, the underlying problems, whether they are differential equations or integral equations, can be translated into a system of algebraic equations. This reduction simplifies the computational burden and facilitates efficient numerical solutions. The sparsity of wavelet representations makes computations more efficient. Since only a small subset of coefficients is required to represent a signal, algorithms based on wavelets can be computationally faster than methods that use non-sparse representations. This is particularly advantageous in applications such as signal processing and image compression. The reduction to algebraic equations, computational efficiency, ease of implementation, and the rapid combination of algorithms make wavelet basis functions a powerful tool in various applications, contributing to their widespread use in scientific, engineering, and computational domains. One of the important aspects of wavelet analysisis the ability to explicitly illustrate and represent other operators and functions through wavelet basis functions. When wavelets are used as basis functions, they provide a way to analyze and represent functions in a multi-resolution fashion, allowing for efficient and flexible representation of signals and operators. Other operators and functions can be explicitly illustrated using wavelets, after which they become apparent in continuous time as $\nu_{ij}(\rho)$ basis functions. A function's set contains a linearly independent set(basis) that spans the entire space. The basis of the set of functions generates all permissible functions, say $h(\rho)$ downsides

$$h(\rho) = \sum_{i,j} \beta_{ij}\nu_{ij}(\rho), \text{where } \ \beta_{i,j} = \langle h, \nu_{ij}\rangle.$$

The functions $\nu_{ij}(\rho)$ are built from a single mother wavelet $\nu(\rho) \in L^2[0,1]$, which is a small pulse, which is a unique property of the wavelet basis. The development of the integration's operational matrix is a critical job in Fredholm *(IDEs)* numerical findings. Many matrix approaches are mentioned in the literature, as mentioned here: *CAS* wavelet operational matrix [4], integral and integro-differential equations [18] and Abel's integral equations [16], Bernoulli wavelet [17], Legendre wavelets operational matrix [19], Haar wavelets operational matrix [7], Laguerre wavelets [10] and Hermite wavelet method for solving integro-differential equations [13]. This work investigates a unique operational integration matrix for the Taylor wavelet-assisted numerical solution of *IDEs*. Additionally, some wavelet-based numerical methods can be found in [22, 21].

2 Definitions and Preliminaries

2.1 Wavelets

A family of functions known as wavelets is generated by dilatating and translating a single function known as the mother wavelet. We have the following family of continuous wavelets when the dilation variable x and the translation variable y vary continuously.

$$\nu_{x,y}(\rho) = |x|^{-\frac{1}{2}}\nu\left(\frac{\rho - y}{x}\right), \quad x, y \in \mathbb{R}, \quad x \neq 0.$$

Discrete wavelets family is defined by restricting the variables x and y to discrete quantities like $x = x_0^{-\Theta}, y = \omega y_0 x_0^{-\Theta}, x_0 > 1$, and $y_0 > 1$, where ω and Θ are natural numbers.

$$\nu_{\Theta,\omega}(\rho) = \left|x_0^{-\Theta}\right|^{\frac{-1}{2}}\nu\left(\frac{\rho - \omega y_0 x_0^{-\Theta}}{x_0^{-\Theta}}\right) = |x_0|^{\frac{\Theta}{2}}\nu\left(x_0^{\Theta}\rho - \omega y_0\right),$$

where $\nu_{\Theta,\omega}(\rho)$ is a basis(wavelet basis) of $L^2(\mathbb{R})$.

2.2 Taylor Wavelets

Four arguments exist for Taylor wavelets $\nu_{\omega,r}(\rho) = \nu(\Theta, \hat{\omega}, r, \rho)$: $\hat{\omega} = \omega - 1, \omega = 1, 2, \ldots, 2^{\Theta-1}$. When Taylor polynomials have order r, we define them as follows on the range $[0, 1]$.

$$\nu_{\omega,r}(\rho) = \begin{cases} 2^{\frac{\Theta-1}{2}} \tilde{L}_r\left(2^{\Theta-1}\rho - \hat{\omega}\right), & \frac{\hat{\omega}}{2^{\Theta-1}} \leq \rho < \frac{\hat{\omega}+1}{2^{\Theta-1}} \\ 0, & \text{otherwise} \end{cases} \tag{2.1}$$

with

$$\tilde{L}_r(\rho) = \sqrt{2r+1} L_r(\rho),$$

where $r = 0, 1, 2, \ldots, \mu - 1$ and $\omega = 1, 2, \ldots, 2^{\Theta-1}$. The coefficient $\sqrt{2r+1}$ is for normality, the dilation parameter is $a = 2^{-(\Theta-1)}$ and the translation parameter is $b = \hat{\omega} 2^{-(\Theta-1)}$. Here, $L_r(\rho)$ are the well-known Taylor polynomials of order r which form a complete basis over the interval $[0, 1]$, which are defined by $L_r(\rho) = \rho^r$[20].

2.3 Approximation Technique

Any function $\Lambda(\rho) \in L^2[0, 1]$ can be expressed in terms of the Taylor wavelet basis in the following way:

$$\Lambda(\rho) = \sum_{\omega=1}^{\infty} \sum_{r=0}^{\infty} g_{\omega,r} \nu_{\omega,r}(\rho)$$

and consider the truncated series of approximation for $\Lambda(\rho)$,

$$\Lambda(\rho) \simeq \sum_{\omega=1}^{2^{\Theta-1}} \sum_{r=0}^{\mu-1} g_{\omega,r} \nu_{\omega,r}(\rho) = E^{\intercal} \nu(\rho) = \Lambda_n(\rho) \tag{2.2}$$

where $\intercal$ indicates transposition, and $E, \nu(\rho)$ are $n \times 1$ $\left(n = 2^{\Theta-1}\mu\right)$ matrices given as

$$E = \left[g_{1,0}, g_{1,1}, \ldots, g_{1,\mu-1}, g_{2,0}, \ldots, g_{2,\mu-1}, \ldots, g_{2^{\Theta-1},\mu-1}, \ldots, g_{2^{\Theta-1},\mu-1}\right]^{\intercal}, \tag{2.3}$$

$$\nu(\rho) = \left[\nu_{1,0}(\rho), \nu_{1,1}(\rho), \ldots, \nu_{1,\mu-1}(\rho), \nu_{2,0}(\rho), \ldots, \nu_{2,\mu-1}(\rho), \ldots, \nu_{2^{\Theta-1},0}(\rho), \ldots, \nu_{2^{\Theta-1},\mu-1}(\rho)\right]^{\intercal}. \tag{2.4}$$

3 Convergence analysis

In this section, two new theorems have been established for the proposed method's convergence analysis as well as error estimation in the following form:

Theorem 3.1 *Let $\Lambda(\rho) \in L^2(\mathbb{R})$ be a continuous function on the interval $[0, 1)$ such that it is bounded by m i.e. $|\Lambda(\rho)| < m$, for every $\rho \in [0, 1)$. Then, the Taylor wavelet coefficients of $\Lambda(\rho)$ in Eq. (2.2) are bounded as:*

$$|g_{\omega,r}| < \frac{\lambda}{2^{\frac{\Theta-1}{2}}} m \frac{2}{2r+1},$$

where m is a constant and λ is given by

$$\lambda = \sqrt{2r+1}.$$

Proof. Using Taylor wavelets, any arbitrary function $\Lambda(\rho)$ can be approximated as:

$$\Lambda(\rho) \simeq \sum_{\omega=1}^{2^{\Theta-1}} \sum_{r=0}^{\mu-1} g_{\omega,r} \nu_{\omega,r}(\rho) = E^T \nu(\rho) = \Lambda_n(\rho), \tag{3.1}$$

where E and $\nu(\rho)$ are given in Eq. (2.3), (2.4) and the coefficients $g_{\omega,r}$ are determined as:

$$g_{\omega,r} = \langle \Lambda, \nu_{\omega,r} \rangle = \int_0^1 \Lambda(\rho) \nu_{\omega,r}(\rho) d\rho = 2^{\frac{\Theta-1}{2}} \sqrt{2r+1} \int_{\frac{\omega-1}{2^{\Theta-1}}}^{\frac{\omega}{2^{\Theta-1}}} \Lambda(\rho) L_r\left(2^{\Theta-1}\rho - \omega + 1\right) d\rho. \tag{3.2}$$

Using the definition of Taylor wavelets $\nu_{\omega,r}(\rho)$, we have

$$\nu_{\omega,r}(\rho) = 2^{\frac{\Theta-1}{2}} \sqrt{2r+1} L_r\left(2^{\Theta-1}\rho - \omega + 1\right), \quad \frac{\omega-1}{2^{\Theta-1}} \leq \rho < \frac{\omega}{2^{\Theta-1}}. \tag{3.3}$$

Let $\lambda = \sqrt{2r+1}$. Let $2^{\Theta-1}\rho - \omega + 1 = x$, then Eq. (3.2) becomes

$$g_{\omega,r} = \frac{\lambda}{2^{\frac{\Theta-1}{2}}} \int_0^1 \Lambda\left(\frac{x+\omega-1}{2^{\Theta-1}}\right) L_r(x) dx.$$

Therefore,

$$|g_{\omega,r}| \leq \frac{\lambda}{2^{\frac{\Theta-1}{2}}} \int_0^1 \left|\Lambda\left(\frac{x+\omega-1}{2^{\Theta-1}}\right)\right| |L_r(x)|\, dx. \tag{3.4}$$

Seeing the properties of Taylor polynomials, we can say that

$$\int_0^1 |L_r(v)|\, dv < \frac{2}{2r+1}, \quad r > 0. \tag{3.5}$$

Using the assumption $|\Lambda(\rho)| < m$ in Eqs. (3.5) and (3.4), we have

$$|g_{\omega,r}| < \frac{1}{2^{\frac{\Theta-1}{2}}} m \frac{2}{\sqrt{2r+1}}. \tag{3.6}$$

Thus the proof of Theorem 3.1 has been completed. Also, boundedness of the function implies absolutely convergent of the series $\Lambda(\rho) = \sum_{\omega=1}^{\infty}\sum_{r=0}^{\infty} g_{\omega,r}$. Hence the Taylor wavelet approximation of the function $\Lambda(\rho)$ is absolutely convergent.

Theorem 3.2 *Let $\Lambda(\rho) \in L^2(\mathbb{R})$ be a continuous function on the interval $[0,1)$ and $|\Lambda(\rho)| < m$ for every $\rho \in [0,1)$. Let $\Lambda^*(\rho) = \sum_{\omega=1}^{2^{\Theta-1}}\sum_{r=0}^{\mu-1} g_{\omega,r}\nu_{\omega,r}(\rho)$ be the Taylor wavelet series expansions where $g_{\omega,r}$, $\nu_{\omega,r}(\rho)$ be the Taylor wavelet coefficients and Taylor wavelet basis respectively. Then, the bound of the truncated error $e(\rho)$ is given as:*

$$\|e(\rho)\|_2 = \|\Lambda(\rho) - \Lambda^*(\rho)\| < \left(\sum_{\omega=2^{\Theta-1}+1}^{\infty}\sum_{r=0}^{\mu-1} g_{\omega,r}^2\right)^{\frac{1}{2}} + \left(\sum_{\omega=1}^{\infty}\sum_{r=\mu}^{\infty} g_{\omega,r}^2\right)^{\frac{1}{2}},$$

where,

$$g_{\omega,r} = \frac{\lambda}{2^{\frac{\Theta-1}{2}}} m \frac{2}{2r+1},\ \lambda = \sqrt{2r+1}.$$

Proof. Any function $\Lambda \in L^2[0,1)$ can be expanded in terms of Taylor wavelets as:

$$\Lambda(\rho) = \sum_{\omega=1}^{\infty}\sum_{r=0}^{\infty} g_{\omega,r}\nu_{\omega,r}(\rho).$$

If $\Lambda^*(\rho)$ is the expansion truncated by using Taylor wavelets, then the error obtained by truncating the above function can be computed as:

$$e(\rho) = \Lambda(\rho) - \Lambda^*(\rho) = \sum_{\omega=2^{\Theta-1}+1}^{\infty}\sum_{r=0}^{\mu-1} g_{\omega,r}\nu_{\omega,r}(\rho) + \sum_{\omega=1}^{\infty}\sum_{r=\mu}^{\infty} g_{\omega,r}\nu_{\omega,r}(\rho). \tag{3.7}$$

From Eq. (3.7), we can write

$$\begin{aligned}\|e(\rho)\| &\leq \left\|\sum_{\omega=2^{\Theta-1}+1}^{\infty}\sum_{r=0}^{\mu-1} g_{\omega,r}\nu_{\omega,r}(\rho)\right\| + \left\|\sum_{\omega=1}^{\infty}\sum_{r=\mu}^{\infty} g_{\omega,r}\nu_{\omega,r}(\rho)\right\| \\ &= \left(\int_0^1 \left|\sum_{\omega=2^{\Theta-1}+1}^{\infty}\sum_{r=0}^{\mu-1} g_{\omega,r}\nu_{\omega,r}(\rho)\right|^2 d\rho\right)^{\frac{1}{2}} + \left(\int_0^1 \left|\sum_{\omega=1}^{\infty}\sum_{r=\mu}^{\infty} g_{\omega,r}\nu_{\omega,r}(\rho)\right|^2 d\rho\right)^{\frac{1}{2}} \\ &\leq \left(\sum_{\omega=2^{\Theta-1}+1}^{\infty}\sum_{r=0}^{\mu-1} |g_{\omega,r}|^2 \int_0^1 |\nu_{\omega,r}(\rho)|^2\, d\rho\right)^{\frac{1}{2}} + \left(\sum_{\omega=1}^{\infty}\sum_{r=\mu}^{\infty} |g_{\omega,r}|^2 \int_0^1 |\nu_{\omega,r}(\rho)|^2\, d\rho\right)^{\frac{1}{2}}.\end{aligned} \tag{3.8}$$

From Theorem 3.1, using the property

$$|g_{\omega,r}| < \frac{\lambda}{2^{\frac{\Theta-1}{2}}} m \frac{2}{2r+1},$$

Eq. (3.8) reduces to

$$\|e(\rho)\|_2 < \left(\sum_{\omega=2^{\Theta-1}+1}^{\infty} \sum_{r=0}^{\mu-1} |g_{\omega,r}|^2 \int_0^1 |\nu_{\omega,r}(\rho)|^2 \, d\rho \right)^{\frac{1}{2}} + \left(\sum_{\omega=1}^{\infty} \sum_{r=\mu}^{\infty} |g_{\omega,r}|^2 \int_0^1 |\nu_{\omega,r}(\rho)|^2 \, d\rho \right)^{\frac{1}{2}}. \tag{3.9}$$

Let us define

$$d_{\omega,r} = \frac{\lambda}{2^{\frac{\Theta-1}{2}}} m \frac{2}{2r+1}. \tag{3.10}$$

Then from Eqs. (3.9) and (3.10), we get

$$\|e(\rho)\|_2 < \left(\sum_{\omega=2^{\Theta-1}+1}^{\infty} \sum_{r=0}^{\mu-1} |d_{\omega,r}|^2 \int_0^1 |\nu_{\omega,r}(\rho)|^2 \, d\rho \right)^{\frac{1}{2}} + \left(\sum_{\omega=1}^{\infty} \sum_{r=\mu}^{\infty} |d_{\omega,r}|^2 \int_0^1 |\nu_{\omega,r}(\rho)|^2 \, d\rho \right)^{\frac{1}{2}}. \tag{3.11}$$

Therefore,

$$\|e(\rho)\|_2 < \left(\sum_{\omega=2^{\Theta-1}+1}^{\infty} \sum_{r=0}^{\mu-1} d_{\omega,r}^2 \int_0^1 |\nu_{\omega,r}(\rho)|^2 \, d\rho \right)^{\frac{1}{2}} + \left(\sum_{\omega=1}^{\infty} \sum_{r=\mu}^{\infty} d_{\omega,r}^2 \int_0^1 |\nu_{\omega,r}(\rho)|^2 \, d\rho \right)^{\frac{1}{2}}. \tag{3.12}$$

By the definition of Taylor wavelets, we have

$$\nu_{\omega,r}^2(\rho) = 2^{\Theta-1}(2r+1) L_r^2 \left(2^{\Theta-1}\rho - \omega + 1\right), \quad \frac{\omega-1}{2^{\Theta-1}} \le \rho < \frac{\omega}{2^{\Theta-1}}. \tag{3.13}$$

Integrating Eq. (3.13) with respect to ρ, we get

$$\int_0^1 \nu_{\omega,r}^2(\rho) = 2^{\Theta-1}(2r+1) \int_{\frac{\omega-1}{2^{\Theta-1}}}^{\frac{\omega}{2^{\Theta-1}}} L_r^2 \left(2^{\Theta-1}\rho - \omega + 1\right) d\rho. \tag{3.14}$$

Let $2^{\Theta-1}\rho - \omega + 1 = u$, Eq. (3.14) becomes

$$\int_0^1 \nu_{\omega,r}^2(\rho) d\rho = (2r+1) \int_0^1 L_r^2(u) du. \tag{3.15}$$

But the standard definition of Taylor polynomial implies that,

$$\int_0^1 L_r^2(u) du = \int_0^1 u^{2r} du = \frac{1}{2r+1}. \tag{3.16}$$

Substituting Eq. (3.16) in Eq. (3.15), we get

$$\int_0^1 \nu_{\omega,r}^2(\rho) d\rho = 1.$$

Thus Theorem 3.2 has been proved. This theorem also implies consistency and stability of the approximation.

3.1 Integration Matrix of Taylor Wavelets

Let $\nu(\rho)$ be the vector consisting of Taylor wavelets defined in the previous section, then

$$I\nu(\rho) = S\nu(\rho),$$

where I and S are the integral operator and the $n \times n$ operational integration matrix , respectively for $n = 2^{\Theta-1}\mu$. Using the Eq. (2.1) , formulation of the Taylor basis, for $\omega = 1, \cdots, 2^{\Theta-1}$ and $r = 0, 1, \cdots, \mu-1$, we have

$$\begin{aligned} I\left(\nu_{\omega,r}(\rho)\right) &= I\left(2^{\frac{\Theta-1}{2}} \tilde{L}_r \left(2^{\Theta-1}\rho - \hat{\omega}\right) \chi_{\left[\frac{\hat{\omega}}{2^{\Theta-1}}, \frac{\hat{\omega}+1}{2^{\Theta-1}}\right]}(\rho)\right) \\ &= 2^{\frac{\Theta-1}{2}} I\left(\sqrt{2r+1} \left(2^{\Theta-1}\rho - \hat{\omega}\right)^r \chi_{\left[\frac{\hat{\omega}}{2^{\Theta-1}}, \frac{\hat{\omega}+1}{2^{\Theta-1}}\right]}(\rho)\right), \end{aligned} \tag{3.17}$$

where $\chi_{\left[\frac{\hat{\omega}}{2^{\Theta-1}}, \frac{\hat{\omega}+1}{2^{\Theta-1}}\right]}(\rho)$ is the characteristic function defined as

$$\chi_{\left[\frac{\hat{\omega}}{2^{\Theta-1}}, \frac{\hat{\omega}+1}{2^{\Theta-1}}\right]}(\rho) = \begin{cases} 1, & \frac{\hat{\omega}}{2^{\Theta-1}} \le \rho \le \frac{\hat{\omega}+1}{2^{\Theta-1}} \\ 0, & \text{otherwise} \end{cases}$$

and $\hat{\omega} = \omega - 1$. For $\omega = 1$, Eq. (**??**) gives

$$I\left(\nu_{1,r}(\rho)\right) = 2^{\frac{\Theta-1}{2}}\sqrt{2r+12}^{(\Theta-1)r} I\left(\rho^r \chi_{\left[\frac{\hat{\omega}}{2^{\Theta-1}}, \frac{\hat{\omega}+1}{2^{\Theta-1}}\right]}(\rho)\right).$$

Therefore, we can obtain seven Taylor Wavelet basis as follows:

$$\begin{aligned}
\nu_{1,0}(\rho) &= 1,\\
\nu_{1,1}(\rho) &= \sqrt{3}\rho,\\
\nu_{1,2}(\rho) &= \sqrt{5}\rho^2,\\
\nu_{1,3}(\rho) &= \sqrt{7}\rho^3,\\
\nu_{1,4}(\rho) &= \sqrt{9}\rho^4,\\
\nu_{1,5}(\rho) &= \sqrt{11}\rho^5,\\
\nu_{1,6}(\rho) &= \sqrt{13}\rho^6,
\end{aligned}$$

for $\Theta = 1$ and $\mu = n = 7$.
Let $\nu(\rho) = [\nu_{1,0}(\rho), \nu_{1,1}(\rho), \nu_{1,2}(v), \nu_{1,3}(\rho), \nu_{1,4}(\rho), \nu_{1,5}(\rho), \nu_{1,6}(\rho)]$.

Now integrate each element of the above vector with respect to the variable ρ limit taking from 0 to ρ, then represent them as a linear combination of Taylor wavelet basis,

$$\begin{aligned}
\int_0^\rho \nu_{1,0}(\rho)d\rho &= \left[\begin{array}{ccccccc} 0 & \frac{1}{\sqrt{3}} & 0 & 0 & 0 & 0 & 0 \end{array}\right]\nu_7(\rho),\\
\int_0^\rho \nu_{1,1}(\rho)d\rho &= \left[\begin{array}{ccccccc} 0 & 0 & \frac{\sqrt{3}}{2\sqrt{5}} & 0 & 0 & 0 & 0 \end{array}\right]\nu_7(\rho),\\
\int_0^\rho \nu_{1,2}(\rho)d\rho &= \left[\begin{array}{ccccccc} 0 & 0 & 0 & \frac{\sqrt{5}}{3\sqrt{7}} & 0 & 0 & 0 \end{array}\right]\nu_7(\rho),\\
\int_0^\rho \nu_{1,3}(\rho)d\rho &= \left[\begin{array}{ccccccc} 0 & 0 & 0 & 0 & \frac{\sqrt{7}}{4\sqrt{9}} & 0 & 0 \end{array}\right]\nu_7(\rho),\\
\int_0^\rho \nu_{1,4}(\rho)d\rho &= \left[\begin{array}{ccccccc} 0 & 0 & 0 & 0 & 0 & \frac{\sqrt{9}}{5\sqrt{11}} & 0 \end{array}\right]\nu_7(\rho),\\
\int_0^\rho \nu_{1,5}(\rho)d\rho &= \left[\begin{array}{ccccccc} 0 & 0 & 0 & 0 & 0 & 0 & \frac{\sqrt{11}}{6\sqrt{13}} \end{array}\right]\nu_7(\rho),\\
\int_0^\rho \nu_{1,6}(\rho)d\rho &= \left[\begin{array}{ccccccc} 0 & 0 & 0 & 0 & 0 & 0 & 0 \end{array}\right]\nu_7(\rho) + \frac{\sqrt{13}}{7\sqrt{15}}\overline{\nu_{1,7}}(\rho).
\end{aligned}$$

Thus, we have $\int_0^\rho \nu(\rho)d\rho = S_{7\times 7}\nu_7(\rho) + \overline{\nu_7}(\rho)$. where,

$$S_{7\times 7} = \left[\begin{array}{ccccccc}
0 & \frac{1}{\sqrt{3}} & 0 & 0 & 0 & 0 & 0\\
0 & 0 & \frac{\sqrt{3}}{2\sqrt{5}} & 0 & 0 & 0 & 0\\
0 & 0 & 0 & \frac{\sqrt{5}}{3\sqrt{7}} & 0 & 0 & 0\\
0 & 0 & 0 & 0 & \frac{\sqrt{7}}{4\sqrt{9}} & 0 & 0\\
0 & 0 & 0 & 0 & 0 & \frac{\sqrt{9}}{5\sqrt{11}} & 0\\
0 & 0 & 0 & 0 & 0 & 0 & \frac{\sqrt{11}}{6\sqrt{13}}\\
0 & 0 & 0 & 0 & 0 & 0 & 0
\end{array}\right].$$

Here, S is defined to be the operational integration matrix of order 7×7, and

$$\overline{\nu_7}(\rho) = \begin{bmatrix} 0 \\ 0 \\ 0 \\ 0 \\ 0 \\ 0 \\ \frac{\sqrt{13}}{7\sqrt{15}}\overline{\nu_{1,7}}(\rho) \end{bmatrix}.$$

This Operational Integration Matrix of Taylor Wavelet basis *(OIMTW)* can also be produced using the same technique for all other values of n.

4 Proposed method for solving the Integro-Diferential Equations *(IDEs)*

Let,

$$\Lambda'(\rho) = h(\rho, \Lambda) + \int_0^1 \kappa(\rho, \xi, \Lambda(\xi))d\xi \tag{4.1}$$

be the integro-differential equation having the initial condition $\Lambda(0) = \delta$. Here, $h(\rho, \Lambda)$ is a continuous function and δ is a constant.

Now we use the Taylor wavelet bases to approximate the highest derivative appearing in the given IDEs as follows,

$$\Lambda'(\rho) = E^{\intercal}\nu(\rho), \tag{4.2}$$

here $\Theta = 1$ and $r = 0, 1, \ldots \mu - 1$, where,

$$E^{\intercal} = [g_{1,0}, g_{1,1}, \ldots, g_{1,\mu-1}],$$
$$\nu(\rho) = [\nu_{1,0}, \nu_{1,1}, \ldots, \nu_{1,\mu-1}]^{\intercal}.$$

Apply integration on both sides of Eq. (4.2) concerning ρ limit from 0 to ρ.

$$\begin{aligned} \Lambda(\rho) &= \Lambda(0) + E^{\intercal}[S\nu(\rho) + \overline{\nu(\rho)}] \\ &= \delta + E^{\intercal}[S\nu(\rho) + \overline{\nu(\rho)}]. \end{aligned} \tag{4.3}$$

Substituting Eq. (4.2) and (4.3) in (4.1), we have

$$E^{\intercal}\nu(\rho) = h\left(\rho, \left(\delta + E^{\intercal}[S\nu(\rho) + \overline{\nu(\rho)}]\right)\right) + \int_0^1 \kappa\left(\rho, \xi, \left(\delta + E^{\intercal}[S\nu(\xi) + \overline{\nu(\xi)}]\right)\right) d\xi. \tag{4.4}$$

Collocate Eq. (4.4), n number of algebraic equations followed by using grid points $\rho_i = \frac{2i-1}{2n}$, where $i = 0, 1, 2, \ldots, n$. Solving these n equations with a suitable method provides Taylor wavelet coefficients. The required numerical solution will next be presented by substituting these coefficients in Eq.(4.3)

5 Quantitive Testings

We present several problems from the field and confirm the productivity as well as the accuracy of the findings to assess the method's efficacy:

$$\mathrm{Y} = \|\Lambda_e(\rho_i) - \Lambda_a(\rho_i)\|_2 = \sqrt{\sum_{i=1}^{n} [\Lambda_e(\rho_i) - \Lambda_a(\rho_i)]^2},$$

where Λ_e is the approximate solution, Λ_a is the accurate solution and Y is denoting the absolute error. The following illustrative problems show the presented method's efficiency, accuracy, and validity with respect to other existing methods.

Problem 5.1 Let

$$\begin{cases} \Lambda'(\rho) = \rho e^{\rho} + e^{\rho} - \rho + \int_0^1 \rho\Lambda(\xi)d\xi \\ \Lambda(0) = 0, \end{cases} \tag{5.1}$$

be the *IDEs* [2, 4, 5, 6, 8, 15, 20]. $\Lambda(\rho) = \rho e^{\rho}$ is the precise solution *(PS)* of this problem. When utilizing the present approach to solve Eq. (5.1), the accuracy of the current approach depends on the size n of the matrix of integration. Comparison between the solution of Taylor's method (current method) or *TS* and the precise solution is shown in Table 5.1, whereas absolute error *(AE)* is shown in Table 5.2. Finally, Table 5.3 shows the numerical findings obtained by the current approach and compared to one of the existing approaches

[4]. Table 5.4 compares the absolute inaccuracy of the current procedure to that of other methods. Fig. 5.1 describes a geometrical interpretation of numerical values of the current method with precise solutions. In Fig. 5.2, error variation for different values of n for the current approach can be observed.

***Table* 5.1:** Value comparison between the current approach *(TS)* and the accurate solution for the Problem 5.1

ρ	*TS at n=6*	*TS at n=7*	*TS at n=8*	*TS at n=9*	*Precise solution*
0	0	0	0	0	0
0.1	0.110517248729256	0.110517084061229	0.110517092019904	0.110517091798469	0.110517091807565
0.2	0.244280532997289	0.244280546432053	0.244280551607897	0.244280551621848	0.244280551632034
0.3	0.404957540507024	0.404957630933154	0.404957642172328	0.404957642254503	0.404957642272801
0.4	0.596729754231302	0.596729861627843	0.596729878676599	0.596729879030421	0.596729879056508
0.5	0.824360295875318	0.824360613332353	0.824360634706961	0.824360635310779	0.824360635350064
0.6	1.093270675744187	1.093271244789225	1.093271279256232	1.093271280183089	1.093271280234305
0.7	1.409626449015646	1.409626852859123	1.409626893661343	1.409626895155630	1.409626895229334
0.8	1.780431778417886	1.780432706086411	1.780432741677801	1.780432742722952	1.780432742793974
0.9	2.213632903312502	2.213642415993803	2.213642788219453	2.213642799701517	2.213642800041255
1	2.718230515182594	2.718278904461437	2.718281684837148	2.71828182217887	2.718281828459046

***Table* 5.2:** Error variation in the current approach for the Problem 5.2

ρ	*n=6*	*n=7*	*n=8*	*n=9*
0.0	0	0	0	0
0.1	1.56 e-07	0.77 e-8	2.12 e-10	0.90 e-11
0.2	0.18 e-07	0.51 e-8	0.24 e-10	1.01 e-11
0.3	1.01 e-07	1.13 e-8	1.00 e-10	1.82 e-11
0.4	1.24 e-07	1.74 e-8	3.79 e-10	2.60 e-11
0.5	3.39 e-07	2.20 e-8	6.43 e-10	3.92 e-11
0.6	6.04 e-07	3.54 e-8	9.78 e-10	5.12 e-11
0.7	4.46 e-07	4.23 e-8	1.56 e-9	7.37 e-11
0.8	9.64 e-07	3.67 e-8	1.11 e-9	7.10 e-11
0.9	9.89 e-06	3.84 e-7	1.18 e-8	3.39 e-10
1	5.13 e-05	2.92 e-6	1.43 e-7	6.28 e-09

***Table* 5.3:** The current method is compared to an existing method for the Problem 5.1.

ρ	*Precise solution*	*CAS in [4]*	*TS at* n=9	*CAS's AE [4]*	*AE of current approach*
0.1	0.110517091807565	0.00134917637	0.110517091798469	1.09 e-01	0.90 e-11
0.2	0.244280551632034	0.00115960044	0.244280551621848	2.43 e-01	1.01 e-11
0.3	0.404957642272801	0.00567152531	0.404957642254503	3.99 e-01	1.82 e-11
0.4	0.596729879056508	0.05931056450	0.596729879030421	5.37 e-01	2.60 e-11
0.5	0.824360635350064	0.01323307510	0.824360635310779	8.11 e-01	3.92 e-11
0.6	1.093271280234300	0.04392877200	1.093271280183089	1.05 e+00	5.12 e-11
0.7	1.409626895229330	0.01412016240	1.409626895155630	1.40 e+00	7.37 e-11
0.8	1.780432742793970	0.01345141170	1.780432742722952	1.77 e+00	7.10 e-11
0.9	2.213642800041250	0.01320452090	2.213642799701517	2.20 e+00	3.39 e-10

***Table* 5.4:** Comparison between the AE of the current approach with some other methods for the Problem 5.1.

ρ	*CAS's [4]*	*DPE's [5]*	*IHPM's [20]*	*SBM's [2]*	*HWM's [6]*	*HEK's [8]*	AE of TS
0.1	1.34 e-03	1.00 e-02	0.23 e-05	1.01 e-07	1.85 e-06	3.69 e-03	0.90 e-11
0.2	1.15 e-03	0.23 e-05	1.01 e-07	1.30 e-06	1.30 e-06	1.45 e-02	1.01 e-11
0.3	5.67 e-03	2.78 e-02	0.92 e-05	4.82 e-07	1.40 e-06	3.20 e-02	1.82 e-11
0.4	5.93 e-02	5.08 e-02	0.20 e-04	1.01 e-07	2.15 e-06	5.56 e-02	2.60 e-11
0.5	1.32 e-02	7.55 e-02	0.37 e-04	1.61 e-06	5.03 e-07	8.47 e-02	3.92 e-11
0.6	4.39 e-02	9.71 e-02	0.57 e-04	2.30 e-06	2.55 e-06	1.18 e-01	5.12 e-11
0.7	1.41 e-02	1.09 e-01	0.83 e-04	3.09 e-06	2.20 e-06	1.55 e-01	7.37 e-11
0.8	1.34 e-02	1.04 e-01	0.11 e-03	3.97 e-06	2.50 e-06	1.95 e-01	7.10 e-11
0.9	1.32 e-02	6.94 e-02	0.14 e-03	4.99 e-06	3.46 e-06	2.35 e-01	3.39 e-10

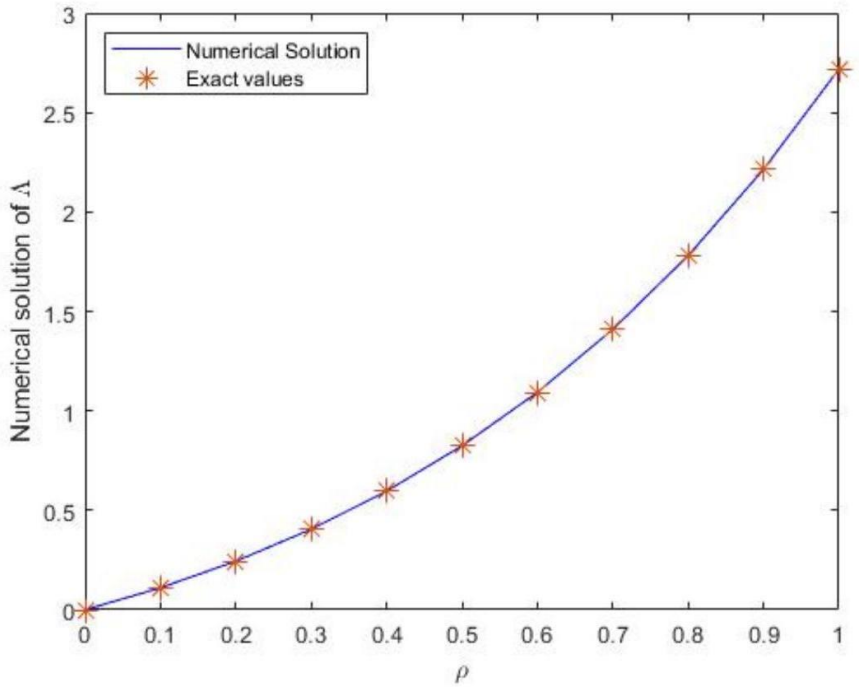

***Figure* 5.1:** Graph representation of the Approximate solution *(TS)* for n=6 and the Precise solution *(PS)* for the Problem 5.1.

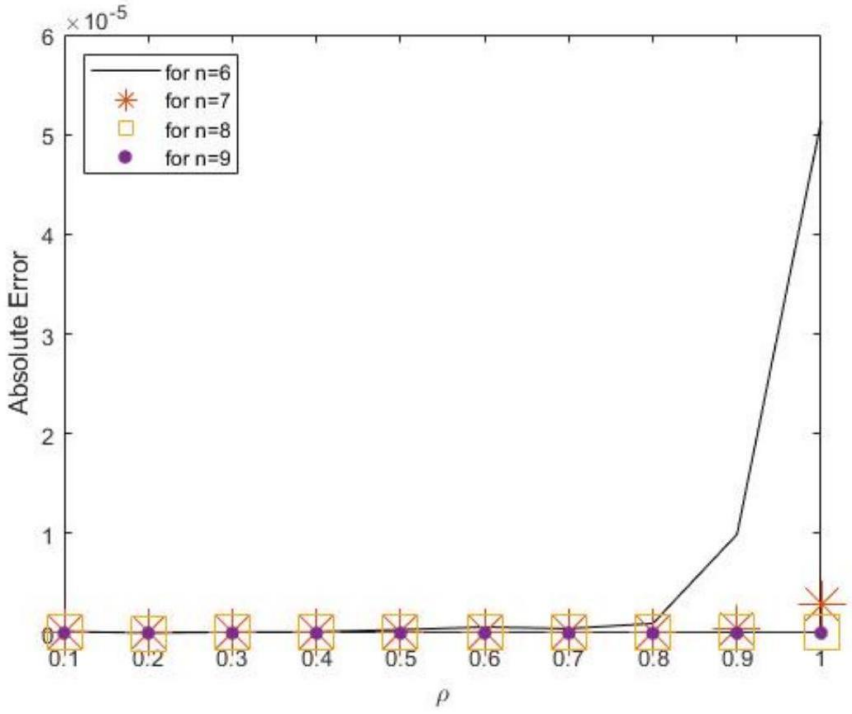

***Figure* 5.2:** Graphical comparison of AE of current method at $n = 6, 7, 8$ and 9 for the Problem 5.1.

Problem 5.2 Let

$$\begin{cases} \Lambda'(\rho) = 1 - \frac{1}{3}\rho + \int_0^1 \rho\xi\Lambda(\xi)d\xi \\ \Lambda(0) = 0. \end{cases} \tag{5.2}$$

be the *IDEs* [2, 4, 5, 6, 8, 15, 20]. $\Lambda(\rho) = \rho$ is the accurate solution of the problem 5.2. Applying the current method at n=10 for solving this problem, we have Ten Taylor wavelet coefficients as follows:

$$\begin{bmatrix} g_{1,0} = 1 \\ g_{1,1} = 0 \\ g_{1,2} = 0 \\ g_{1,3} = 0 \\ g_{1,4} = 0 \\ g_{1,5} = 0 \\ g_{1,6} = 0 \\ g_{1,7} = 0 \\ g_{1,8} = 0 \\ g_{1,9} = 0 \end{bmatrix}$$

The Taylor wavelet solution, which is identical to the analytic solution, is obtained by replacing these coefficients in Eq. (4.3). This problem demonstrates the method's efficiency, applicability, and validity. Numerical values of the solution of problem 5.2 as shown in Table 5.5 obtained in different existing methods and the current method *(TS)* along with the absolute error.

***Table* 5.5:** Numerical comparison of current solution with certain other existing methods for the Problem 5.2.

ρ	*PS*	*CAS [4]*	*TS*	*CAS's AE [4]*	*CAS in [4]*	*DPEM [5]*	*SAM [2]*	*HWM [6]*	*HEK [8]*	*AE of TS*
0.1	0.1	0.00021794238	0.1	9.98 e-02	2.17 e-04	1.60 e-03	3.79 e-06	1.60 e-06	1.50 e-03	0
0.2	0.2	0.00063854821	0.2	1.99 e-01	6.38 e-04	6.09 e-03	1.51 e-05	2.36 e-06	5.36 e-03	0
0.3	0.3	0.00077137049	0.3	2.99 e-01	7.91 e-04	1.32 e-02	3.41 e-05	2.26 e-06	1.06 e-02	0
0.4	0.4	0.02155860050	0.4	3.78 e-01	2.15 e-02	2.29 e-02	6.06 e-05	1.31 e-06	1.65 e-02	0
0.5	0.5	0.00499358429	0.5	4.95 e-01	4.99 e-03	3.51 e-02	9.47 e-05	4.85 e-07	2.21 e-02	0
0.6	0.6	0.02217288150	0.6	5.78 e-01	2.21 e-02	6.69 e-02	1.36 e-05	9.28 e-07	2.67 e-02	0
0.7	0.7	0.00010564545	0.7	7.00 e-01	1.05 e-04	7.12 e-02	1.85 e-04	1.48 e-06	2.95 e-02	0
0.8	0.8	0.00143233681	0.8	7.99 e-01	1.43 e-03	8.63 e-02	2.42 e-04	1.19 e-06	2.98 e-02	0
0.9	0.9	0.02077474610	0.9	8.79 e-01	2.07 e-02	1.08 e-01	3.06 e-04	5.40 e-08	2.71 e-02	0

Problem 5.3 Let

$$\begin{cases} \Lambda'(\rho) = \int_0^1 \sin[4\pi\rho + 2\pi\xi]\Lambda(\xi)d\xi + \Lambda(\rho) - 2\pi\sin(2\pi\rho) - \cos(2\pi\rho) - \frac{1}{2}\sin(4\pi\rho) \\ \Lambda(0) = 1 \end{cases} \tag{5.3}$$

be the *IDEs* [4], $\Lambda(\rho) = \cos(2\pi\rho)$ is the precise answer to this problem. Numerical values obtained in the current method *(TS)* and precise solution are shown in Table 5.6 and compared with an existing method after simplifying Eq. (5.3). The numerical answer is graphically compared to the precise solution in Fig. 5.3. The absolute error that occurred in this problem is compared with an existing method in Fig. 5.4.

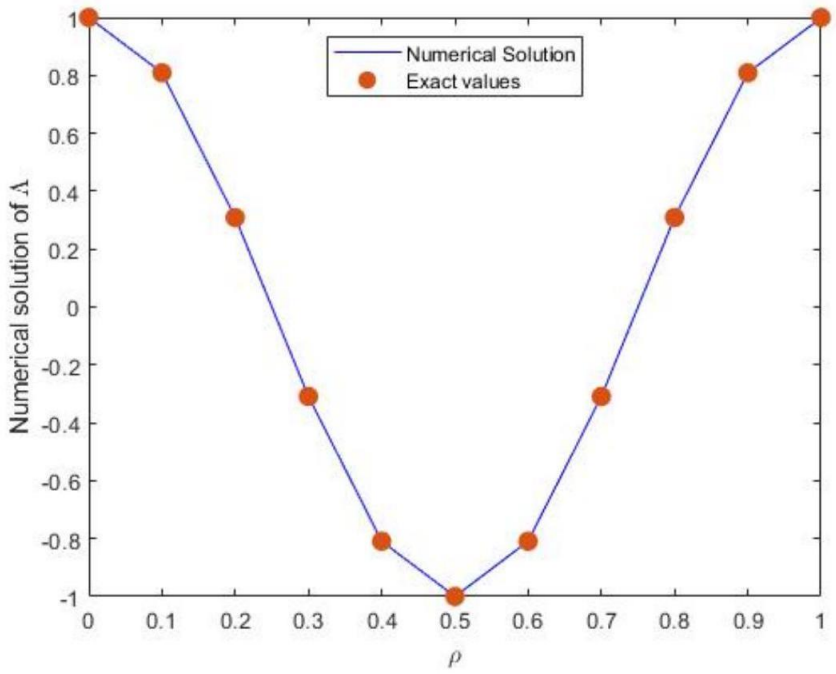

***Figure* 5.3:** Graphical representation of the *TS* for n=10 and the precise solution for the Problem 5.3.

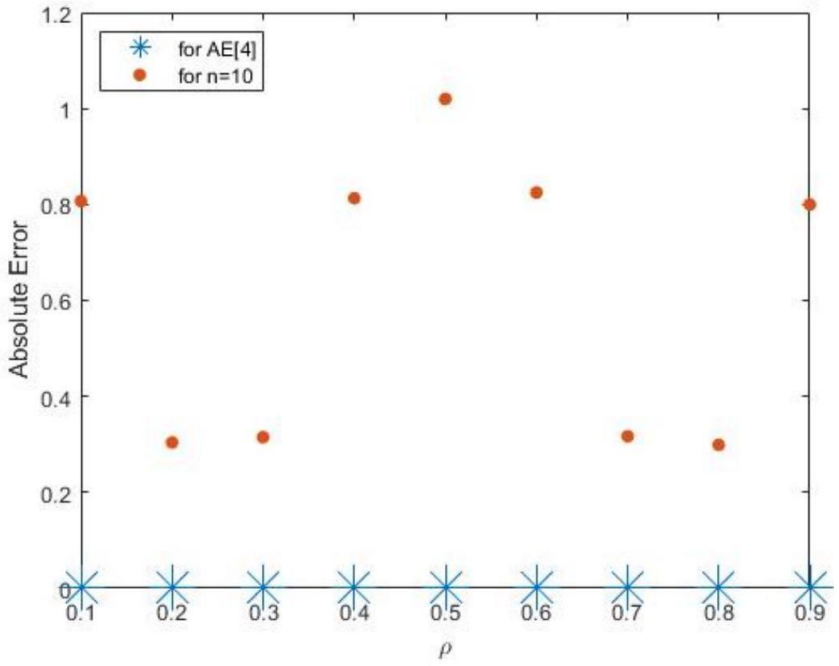

***Figure* 5.4:** Point diagram of absolute errors (AE) for the current method at n=10 and *CAS's* AE[4] for the Problem 5.3.

***Table* 5.6:** Current method is compared with an existing method for the Problem 5.3.

ρ	*PS*	*CAS method in [4]*	*TS at* n=10	*CAS's AE [4]*	*Absolute error of TS*
0.1	0.809016994374947	0.00240432854	0.809022044656112	8.07 e-01	5.05 e-06
0.2	0.309016994374947	0.00507123331	0.309016289100111	3.04 e-01	0.70 e-06
0.3	-0.309016994374948	0.00625477225	-0.309018658682028	3.15 e-01	1.66 e-06
0.4	-0.809016994374947	0.00387315246	-0.809014212286664	8.13 e-01	2.78 e-06
0.5	-1.000000000000000	0.01746016710	-0.999993298619171	1.02 e+00	6.70 e-06
0.6	-0.809016994374947	0.01584825600	-0.809012181620363	8.25 e-01	4.81 e-06
0.7	-0.309016994374948	0.00841721725	-0.309016273658540	3.17 e-01	0.72 e-06
0.8	0.309016994374947	0.00965467633	0.309025332212964	2.99 e-01	8.33 e-06
0.9	0.809016994374947	0.00948709579	0.809005478573982	8.00 e-01	1.15 e-05

Problem 5.4 Let,

$$\Lambda'(\rho) = \frac{5}{4} - \frac{1}{3}\rho^2 + \int_0^1 \left(\rho^2 - \xi\right)(\Lambda(\xi))^2 d\xi, \quad \Lambda(0) = 0, \tag{5.4}$$

be *IDEs* [14, 15].The nonlinear Eq. (5.4) has a precise solution as $\Lambda(\rho) = \rho$. Using the current approach at $n = 3$ to simplify Eq. (5.4), we have Taylor wavelet approximation coefficients as $g_{1,0} = 1, g_{1,1} = 0, g_{1,2} = 0$, obtained by using Newton's iterative technique (taking an initial guess (1,0,0)) in *MATLAB*. Now using these coefficients in Eq.(4.3), We find a solution that is identical to the precise solution. This problem demonstrates the effectiveness of our method. Numerical values and Absolute errors of the current approach are placed in Table 5.6 and can be compared with the precise solution and different known methods [14, 15].

***Table* 5.7:** The current method is compared with some other existing methods for the Problem 5.4.

ρ	*PS*	*TS*	*RHFs [15] at* k = 32	*RHF's AE [15]*	*B-spline's AE* [14] *at* N = 27	*Absolute error of TS*
0.1	0.1	0.1	0.10002	2.0 e-05	1.94 e-14	0
0.2	0.2	0.2	0.20008	8.0 e-05	3.83 e-14	0
0.3	0.3	0.3	0.30007	7.0 e-05	5.05 e-14	0
0.4	0.4	0.4	0.40008	8.0 e-05	6.77 e-14	0
0.5	0.5	0.5	0.50001	1.0 e-05	8.37 e-14	0
0.6	0.6	0.6	0.60001	1.0 e-05	9.30 e-14	0
0.7	0.7	0.7	0.70002	2.0 e-05	10.5 e-14	0
0.8	0.8	0.8	0.80008	8.0 e-05	11.4 e-14	0
0.9	0.9	0.9	0.89991	9.0 e-05	12.1 e-14	0

6 Conclusion

From the above analysis, it is concluded that the Taylor wavelet-based collocation method is much better efficient compared to many different existing methods for numerically solving *IDEs* in numerous disciplines of science and engineering. To get more accurate results, the number of collocation points can be increased.

Acknowledgement. All authors are thankful to the editor and referees for their suggestions to bring the paper in its present form.

References

[1] D. Bahuguna, A. Ujlayan and D. N. Pandey, A comparative study of numerical methods for solving an Integro differential equation, *Comp. Math. Appl.*, **57**(2009), 1485-1493.

[2] M. I. Berenguer, M. V. F. Munoz, A. I. Garralda-Guillem and M. R. Galan, A sequential approach for solving the Fredholmintegro-differential equation, *Appl. Math. Comput.*, **62**(2012), 297-304 .

[3] G. Bier, Y. Öztürk and M. Gülsu, Numerical approach for solving linear Fredholmintegro-differential equation with piecewise intervals by Bernoulli polynomials, *Int. J. Comp. Math.*, **95**(2018), 2100-2111.

[4] H. Danfu and S. Xufeng, Numerical solution of integro-differential equations by using CAS wavelet operational matrix of Integration, *Appl. Math. Comput.*,**194**(2007), 460-466.

[5] P. Darania and A. Ebadian, A method for the numerical solution of the integro-differential equations, *Appl. Math. Comput.*, **188**(2007), 657-668 .

[6] M. Erfanian, M. Gachpazan and H. Beiglo, A new sequential approach for solving the integro-differential equation via haar wavelet bases, *Comput. Math. Math. Phys.*, **57**(2017), 297-305

[7] J. S. Gu and W. S. Jiang, The haar wavelets operational matrix of integration, *Int. J. Systems Sci.*, **27**(1996), 623-628 .

[8] E. Haq, A. S. Khan and M. Ali, An efficient approach for solving the linear and nonlinear integrodifferential equation, *CRPASE*, **06**(2020), 104-107 .

[9] E. Keshavarz, Y. Ordokhani and M. Razzaghi, The Taylor wavelets method for solving the initial and boundary value problems of Bratu-type equations, *Science Direct*, **128**(2018), 205-216

[10] S. Kumbinarasaiah and R. A. Mundewadi, Numerical method for the solution of Abel's integral equations using laguerre wavelet, *J. Inform. Comput. Sci.*, **14**(2019), 250-258 .

[11] H. Kumar, R. C. Singh Chandel and Harish Srivastava, On a fractional non lineaer biological model problem and its approximate solutions through Volterra integral equation, Jnanabha **47**(1) (2017), 143-154.

[12] H Kumar, A class of two variables sequence of functions satisfying Abel's integral equation and the phase shifts, Jnanabha **49** (1)(2019), 89-96.

[13] S. Kumbinarasaiah and R. A. Mundewadi, The new operational matrix of integration for the numerical solution of integro-differential equations via Hermite wavelet, *SeMA Journal*, **78** (2021), 367-384.

[14] Z. Mahmoodi, J. Rashidinia and E. Babolian, B-spline collocation method for linear and nonlinear Fredholm and Volterraintegro-differential equations, *Appl. Anal.*, **92**(2013), 1787-1802.

[15] F. Mirzaee, The RHFs for solution of nonlinear fredholmintegro-differential equations, *Appl. Math. Sci.*, **5**(2011), 3453-3464 .

[16] R. A. Mundewadi and S. Kumbinarasaiah, Numerical solution of Abel's integral equations using Hermite wavelet, *Appl. Math. Nonlinear Sci.*, **4** (2019), 395-406.

[17] B. A. Mundewadi and R.A. Mundewadi, Bernoulli wavelet collocation method for the numerical solution of integral and integro-differential equations, *Int. J. Eng. Sci. Math.*, **7**(2018), 286-305.
[18] R. A. Mundewadi and B. A. Mundewadi, Hermite wavelet collocation method for the numerical solution of integral and integro-differential equations, *Int. J. Math. Trends Technol*, **53**(2018) 215-231.
[19] M. Razzaghi and S. Yousefi, The Legendre wavelets operational matrix of integration, *Int. J. Syst. Sci.*, **32** (2001), 495-502.
[20] E. Yusufoglu, Improved homotopy perturbation method for solving Fredholm type integro-differential equations, *Chaos Solitons Fractals*, **41**(2009), 28-37 .
[21] Vivek, M. Kumar and S. N. Mishra, Solution of linear and nonlinear singular value problems using operational matrix of integration of Taylor wavelets, *J. Taibah Univ. Sci.*, **17**(1) (2023), 2241716.
[22] Vivek, M. Kumar and S. N. Mishra, A fast Fibonacci wavelet-based numerical algorithm for the solution of HIV-infected CD4+ T cells model, *Eur Phys J Plus.*, **138**(5)(2023):458.